RESEARCH ARTICLE

WILEY-VCH

Remote Electronic Effect of Chiral N-Heterocyclic Carbene Catalyst on an Asymmetric Benzoin Reaction

Tsubasa Inokuma,[a,b] Kentaro Hashimoto,[a] Tatsuya Fujiwara,[a] Chunzhao Sun,[a] Satoru Kuwano,[c] and Ken-ichi Yamada*[a,b]

[a]   Dr. T. Inokuma, K. Hashimoto, T. Fujiwara, C. Sun, Prof. Dr. K. Yamada
      Graduate School of Pharmaceutical Sciences
      Tokushima University
      Shomachi, Tokushima 770-8505, Japan.
      E-mail: yamak@tokushima-u.ac.jp
[b]   Dr. T. Inokuma, Prof. Dr. K. Yamada
      Research Cluster on "Key Material Development"
      Tokushima University
      Shomachi, Tokushima 770-8505, Japan.
[c]   Dr. S. Kuwano
      Graduate School of Pharmaceutical Sciences
      Kyoto University
      Yoshida, Sakyo-ku, Kyoto 606-8501, Japan.

      Supporting information for this article is given via a link at the end of the document.

Abstract: A remote electronic effect of chiral aminoindanol-derived N-heterocyclic carbene catalyst on an asymmetric benzoin reaction was investigated. The catalyst bearing remote electron-withdrawing substituents increased enantioselectivity of the reaction at the cost of the reaction rate. DFT calculations rationalized the increased enantioselectivity.

Introduction

A benzoin reaction, hydroacylation of a C=O bond by aldehydes, is a representative N-heterocyclic carbene (NHC)-catalyzed reaction.[1] Since the first report by Ukai and coworkers,[2] efforts have been made for mechanistic investigation[3–6] as well as development of a catalytic asymmetric version.[7–10] Typically, the reaction is a simple dimerization of aldehyde to give α-hydroxy ketones, and thus, has been utilized as a benchmark test for a newly developed chiral NHC catalyst,[11–20] due to the simple operation as well as the ready availability of various aldehydes. In addition, the reaction, especially an intramolecular version, is useful as a synthetic method to give versatile synthetic intermediates, α-hydroxy ketones, and its application to natural product synthesis has been reported.[21–28]

During our research on organocatalyzed reactions,[29–41] we developed the electronic tuning of an aminoindanol-derived chiral NHC[42] by installing a remote electron-withdrawing substituent.[43–45] A common strategy to tune the electron density on NHC is substitution of the *N*-aryl group of NHCs.[22,46–48] The advantage of the remote substitution is that the substituents are located far from the carbene carbon atom, causing less steric or electrostatic interference in reactions.[43] We recently applied the electronically remote-tuned chiral NHCs to an asymmetric intramolecular Stetter reaction and found that the electronic tuning of chiral NHC affected not only the reaction rate but also the enantioselectivity.[49] Herein, we report the remote electronic effect of chiral NHC on the asymmetric benzoin reaction, another typical *Umpolung* reaction of aldehydes.

Results and Discussion

The chiral NHCs derived from **3a** and **3c–e**, as well as reference precatalyst **3b**, were applied to the benzoin reaction of benzaldehyde (**1a**). To a stirred solution of **3b** and 1,8-bis-(dimethylamino)naphthalene (proton sponge) in dichloroethane (1 mol% each), **1a** was added at 0 °C. After 1 h, the reaction was quenched although it was incomplete, and benzoin **2a** was obtained in 56% yield with 93% enantiomeric excess (ee; Table 1, entry 2). With precatalyst **3a**, bearing an electron-donating methyl group, the yield as well as enantioselectivity decreased (29%, 89% ee; entry 1). When electron-deficient precatalyst **3c** was used, the reaction accelerated with comparable enantiose-

Table 1. Remote Electronic Effect on the Reaction of **1a**.[a]
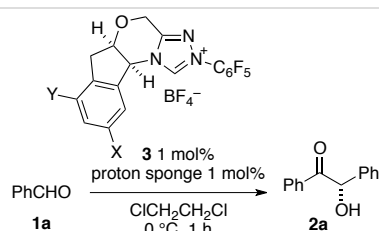
entry	3	X	Y	yield[b]	ee[c]
1	**3a**	Me	H	29	89
2	**3b**	H	H	56	93
3	**3c**	Br	H	65	93
4	**3d**	NO$_2$	H	63	94
5	**3e**	NO$_2$	Br	29	95

[a] The reaction was conducted with **1a** (1 mmol), **3**, and proton sponge (0.01 mmol each) in dichloroethane (1 mL). [b] Isolated yield. [c] Determined by chiral stationary phase HPLC.

lectivity (65%, 93% ee; entry 3). The reaction with **3d**, bearing a more electron-withdrawing nitro group, decreased the yield of **2a** in spite of higher ee (63%, 94% ee, entry 4). The use of more electron-deficient precatalyst **3e** much retarded the reaction to give only 29% of **2a** although the enantioselectivity was improved (95% ee; entry 5).
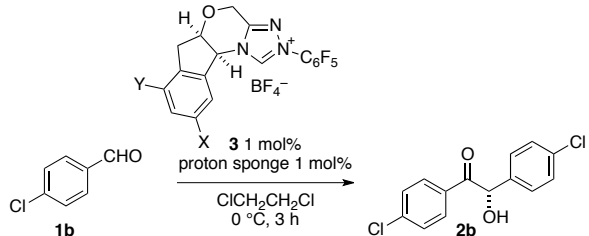
The accepted reaction pathway of the benzoin reaction is shown in Figure 1.[3] NHC **I** undergoes addition to aldehyde **1** (step A) to give tetrahedral intermediate **II**, which tautomerizes into diaminoenol intermediate **III** (step B). The C–C bond formation of **III** and another molecule of **1** proceeds through transition state **IV**, where hydrogen atom transfer occurs from the oxygen atom of **III** to that of **1**, generating intermediate **V** (step C). Finally, regeneration of NHC **I** from **V** provides product **2** (step D). The slower reaction with **3a**, bearing an electron-donating group, indicates that the rate-limiting step of the reaction is step B, in which deprotonation of the carbinol proton of **II** is involved. The electron-withdrawing substituents in **3c**–**3e** are expected to increase the acidity of the carbinol proton.[46,49] In the reaction with **3d**, involving intermediate **II** with a highly acidic carbinol proton, the tautomerization step would not be rate-limiting. Instead, step A or C, involving nucleophilic addition of **I** or **III**, whose nucleophilicities decrease by the electron-withdrawing substituents, are the most probable rate-limiting steps. This speculation is consistent with the previous kinetic study which revealed that the activation energies of steps A, B, and C are of similar levels in the thiazolinylidene-catalyzed reaction, and thus the rate-limiting step is likely interchangeable.[5]

Next, the reaction of electron-deficient benzaldehyde **1b** was examined (Table 2). As in the reaction of **1a**, the reaction with **3a** was also slower than the reference reaction with **3b** (86% yield, 78% ee; entry 2), giving **2b** in 70% yield and 78% ee (entry 1). In contrast to the reaction of **1a**, the reaction of **1b** became slower when more electron-deficient precatalysts **3b**–**e** were used (86, 60, 54, and 48% yield), while the enantioselectivities exhibited the same tendency, *i.e.*, the higher selectivity with the more electron-deficient precatalyst (78, 81, 86, and 86% ee; entries 2–5). These results indicate that step B is not the rate-limiting in the reactions of electron-deficient aldehydes, except for the reaction with electron-donating **3a** (entry 1), and thus the reactions with electron-deficient precatalysts **3c**–**3e** became slower by the decreased nucleophilicity of NHCs **I** and/or more

acidic than that derived from **1a**.intermediate **III** (entries 3–5). This speculation seems to be reasonable because intermediate **II** derived from **1b** is likely

Next, the reaction of electron-rich benzaldehyde **1c** was examined (Table 3). The reaction was much slower than those of **1a** and **1b**, probably due to reduced electrophilicity of the aldehyde and weakened acidity of intermediate **II**, which retard all the potential rate-limiting steps A, B, and C. Nevertheless, the substituent effect of the catalyst on the reaction of **1c** showed the same tendency as that of **1a**. The yield was the highest with **3c** bearing a bromo atom (35%, entry 3) and became lower as
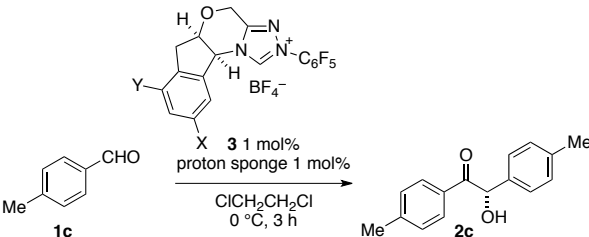
Table 2. Remote Electronic Effect on the Reaction of **1b**.[a]

entry	3	X	Y	yield[b]	ee[c]
1	**3a**	Me	H	70	78
2	**3b**[d]	H	H	86	78[e]
3	**3c**	Br	H	60	81
4	**3d**	NO$_2$	H	54	86
5	**3e**	NO$_2$	Br	48	86

[a] The reaction was conducted with **1b** (2 mmol), **3**, and proton sponge (0.02 mmol each) in dichloroethane (2 mL). [b] Isolated yield. [c] Determined by chiral stationary phase HPLC. [d] Antipode was used. [e] Antipode was obtained.

Table 3. Remote Electronic Effect on the Reaction of **1c**.[a]

entry	3	X	Y	yield[b]	ee[c]
1	**3a**	Me	H	8	90
2	**3b**	H	H	23	93
3	**3c**	Br	H	35	93
4	**3d**	NO$_2$	H	32	94
5	**3e**	NO$_2$	Br	28	95

[a] The reaction was conducted with **1c** (0.85 mmol), **3**, and proton sponge (8.5 µmol each) in dichloroethane (0.85 mL). [b] Isolated yield. [c] Determined by chiral stationary phase HPLC.
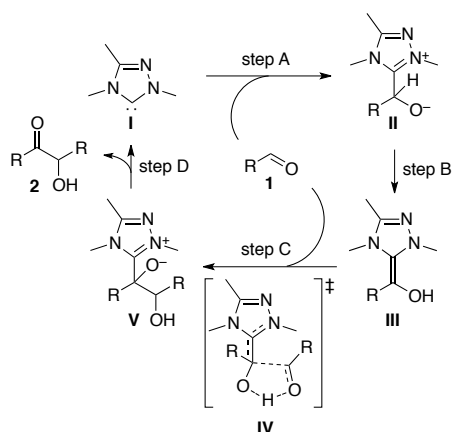

Figure 1. The Accepted Reaction Pathway of the Benzoin Reaction.

the electron density on the catalyst either increased or decreased (8–32%, entries 1, 2, 4, and 5), while the enantioselectivity improved as the electron density on the catalyst decreased (90–95% ee, entries 1–5).
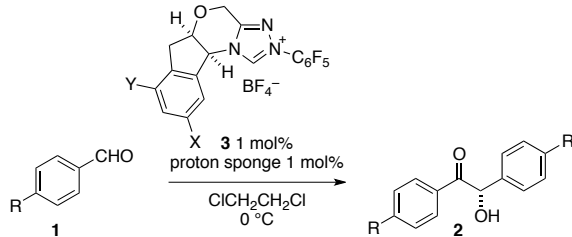
Although it was unexpected, the above results clearly show the advantage of electron-deficient chiral NHCs derived from **3d** and **3e** for improving the enantioselectivity at the cost of reaction rate. To examine the generality, the effects of the electron-withdrawing substituents were investigated on other benzaldehyde derivatives (Table 4). In the reactions of electron-deficient **1b–e**, products **2b–e** were obtained with lower enantioselectivity than the reactions of **1a** but the enantioselectivity was clearly improved by using **3d**, bearing a nitro group, in place of non-substituted precatalyst **3b** (89 vs 80% ee, 76 vs 66% ee, and 72 vs 42% ee; entries 4 vs 3, 6 vs 5, and 10 vs 8). Although the reaction was slower with **3d** or **3e** than **3b**, products **2a–e** were produced in good to excellent

yields (69%–quant) with prolonged reaction time (entries 4, 6, and 10) and increased amount of the catalyst (5 mol%) in the r eaction of **1a** (entry 2). It is noteworthy that racemization of the product was observed in the reaction of **1e**, bearing strongly electron-withdrawing trifluoromethyl group; that is, the product with higher enantiomeric excess was obtained after 5 min than after 3 h (57 vs 42% ee, entries 7 and 8) when **3b** was used as a catalyst. The use of less basic NHC derived from **3d** is likely beneficial to prevent the racemization; the difference of ee wasnegligible with **3d** between the reactions for 15 min and 3 h (73 vs 72% ee, entries 9 and 10). In the reactions of **1b–e**, the most electron-deficient precatalyst **3e** failed to further improve the enantioselectivity and only retarded the reactions.

The reactions of electron-rich benzaldehyde derivatives **1c** and **1f** were much slower, and satisfactory yield was not realized even with prolonged reaction time. Thus, the reactions were conducted with increased amount of the precatalyst (5 mol%) without solvent[50] which gave the products in good to excellent yield (75–98%). As expected, the reactions with electron-deficient precatalyst **3e** provided the products in higher enantioselectivity than those with non-substituted precatalyst **3b** (93 vs 89% ee and 94 vs 92% ee, entries 12 vs 11 and 14 vs 13).

To gain insight into the increased enantioselectivity with electron-deficient chiral NHCs, DFT calculations were performed for the reaction of benzaldehyde (**1a**) with **3b** (X = H). The transition state (TS) search for the enantio-determining step (**IV** in Figure 1) at the B3LYP-D3/6-311+G**//B3LYP/6-31G* theoretical level with solvation corrections using the Polarizable Continuum Model (PCM) provided TS$_{major}$ and TS$_{minor}$ ($\Delta G^{\ddagger}$ 11.9 and 13.7 kcal/mol) as the lowest-energy TS geometries to give **2a** and *ent*-**2a**, respectively (Figure 2). In these geometries, the diaminoenol moiety has *E*-configuration, in which π-π interaction is likely present between the phenyl ring and the perfluorophenyl ring, and the reacting aldehyde is on the less-hindered *si*-face of the diaminoenol. The carbonyl oxygen of the aldehyde forms hydrogen-bond with the hydroxy group, which stabilizes the transition states and also activates the electrophilicity of the aldehyde. The substituents on the bond-forming carbon atoms are overlapped, and the phenyl group of the aldehyde is on the same side of the triazolyl group in TS$_{major}$, while it is on the same side of the phenyl group in TS$_{minor}$. These geometries are

Table 4. Benzoin Reactions of **1a–f**.

entry	1/2	R	3/X/Y	time	yield[a]	ee[b]
1[c]	1a/2a	H	3b/H/H	4 h	79	93
2[d]	1a/2a	H	3e/NO₂/Br	8.5 h	83	96
3[e]	1b/2b	Cl	3b/H/H	10 h	94	80
4[e]	1b/2b	Cl	3d/NO₂/H	22 h	80	89
5[f]	1d/2d	CO₂Me	3b/H/H	10 h	87	66
6[f]	1d/2d	CO₂Me	3d/NO₂/H	18 h	69	76
7[g]	1e/2e	CF₃	3b/H/H	5 min	74	57
8[g]	1e/2e	CF₃	3b/H/H	3 h	quant	42
9[g]	1e/2e	CF₃	3d/NO₂/H	15min	81	73
10[g]	1e/2e	CF₃	3d/NO₂/H	3 h	quant	72
11[h]	1c/2c	Me	3b/H/H	4 h	98	89
12[h]	1c/2c	Me	3e/NO₂/Br	21 h	88	93
13[h]	1f/2f	OMe	3b/H/H	6 h	85	92
14[h]	1f/2f	OMe	3e/NO₂/Br	22 h	75	94

[a] Isolated yield. [b] Determined by chiral stationary phase HPLC. [c] With **1a** (1 mmol), and **3** and proton sponge (10 μmol each) in dichloroethane (1 mL). [d] With **1a** (1 mmol), and **3** and proton sponge (50 μmol each) in dichloroethane (1 mL). [e] With **1b** (0.3 mmol), and **3** and proton sponge (3 μmol each) in dichloroethane (0.2 mL). [f] With **1d** (0.5 mmol), and **3** and proton sponge (5 μmol each) in dichloroethane (0.5 mL). [g] With **1e** (1.5 mmol), and **3** and proton sponge (15 μmol each) in dichloroethane (1.5 mL). [h] Without solvent with **1** (0.4 mmol), and 5 mol% of **3** and proton sponge (20 μmol each).
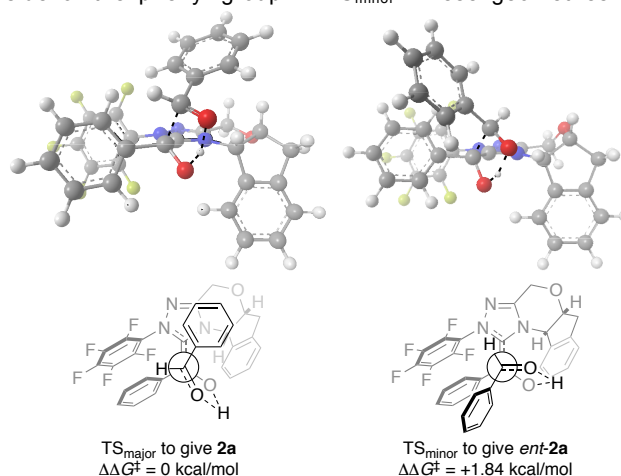
TS$_{major}$ to give **2a**
$\Delta\Delta G^{\ddagger}$ = 0 kcal/mol

TS$_{minor}$ to give *ent*-**2a**
$\Delta\Delta G^{\ddagger}$ = +1.84 kcal/mol

Figure 2. Chem3D Perspective View and Newman Projection of the Transition States.

basically consistent with those reported for a related triazolinylidene NHC at the ONIOM (B3LYP/6-31G*:AM1) theoretical level.[51] The free-energy difference between TS_{major} and TS_{minor} was 1.84 kcal/mol, corresponding to 94% ee at 0 °C, which is consistent with the experimental result (93% ee; Table 1, entry 2). The TS geometries were also calculated for the reactions with **3a** (X = Me) and **3d** (X = NO$_2$) to give free-energy difference of 1.75 and 2.55 kcal/mol, corresponding to 92% ee and 99% ee at 0 °C, respectively, which are in good agreement with the experimental tendency (89% ee and 94% ee; Table 1, entries 1 and 4).

In the literature,[51] the energy difference between the major and minor TS was attributed to the repulsion between the phenyl groups in the minor TS and attractive π-aryl–iminium ion interaction in the major TS. To gain more insight into the origin of enantioselectivity, noncovalent interactions (NCI) in TS were visualized (Figure 3).[52] In both TSs, the π-π interaction between the *N*-perfluorophenyl and the phenyl; and attractive electrostatic interactions between the indane C1 hydrogen and the aldehyde oxygen atoms, and the indane C7 hydrogen and the diaminoenol oxygen atoms were indicated (blue lines, Figure 3). In the minor TS, the red–yellow rich surface between the diaminoenol phenyl and the aldehyde phenyl (red circle, Figure 3 below) indicates the repulsive interaction as speculated in the literature,[51] probably due to non-parallel orientation of the two phenyl rings. However, the previously proposed π-aryl–iminium ion interaction[51] was not supported by this analysis; the surface between the aldehyde phenyl ring and triazole ring in the major TS is also red–yellow rich (red circle, Figure 3 above), indicating that the interaction is also repulsive.
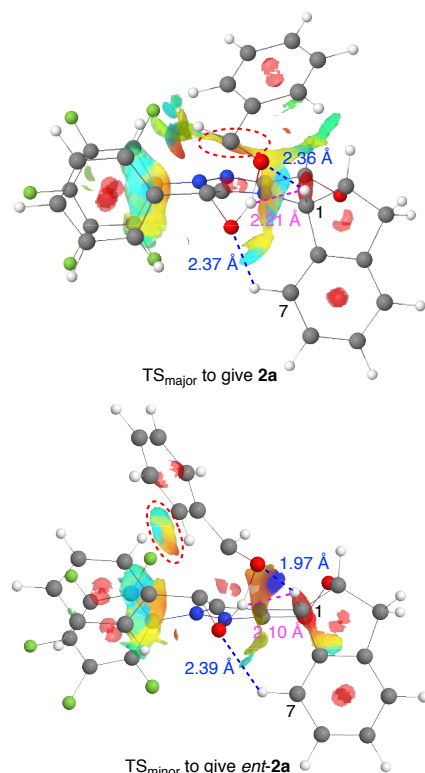
Next, the distortion/interaction analysis was performed (Table 5).[53] The activation energies (E_{act}), the distortion energies of **1a** and intermediate **III** (ΔE_{1a} and ΔE_{III}), and the interaction energy between **1a** and intermediate **III** (E_{int}) were calculated at the B3LYP-D3/6-311+G**//B3LYP/6-31G* theoretical level. The activation energies of the minor TS are the same for **3a** and **3b** (4.3 kcal/mol), while that of the major TS with **3b** is slightly more stable than that with **3a** (0.9 vs 1.2 kcal/mol). This indicates that the decreased enantioselectivity with **3a** (X = Me) could be attributed to destabilization of the major TS; that is, the enantioselectivity decreased with **3a** because of slower production of **2a** rather than faster production of *ent*-**2a**. Comparison of the major TS with **3a** and **3b** shows that the interaction energies are almost the same (–72.4 and –72.3 kcal/mol), while both distortion energies (ΔE_{1a} and ΔE_{III}) are slightly higher for **3a** than those for **3b** (32.7 vs 32.5 and 40.9 vs 40.7 kcal/mol). This probably means that the aldehyde and intermediate **III** need more distortion in the major TS with **3a** to gain stabilizing interaction to the same extent as that with **3b**. This is probably because the electron-donating methyl substituent increases electron density on the indane C1 and C7 hydrogen atoms, and the oxygen atoms of the aldehyde and the diaminoenol need to get closer than those in the major TS with **3b** to form effective hydrogen bonds (Figure 3 above). Actually, the O–H distances are shorter in the major TS with **3a** than in the major TS with **3b** (O–H1: 2.351 vs 2.360 Å, O–H7: 2.365 vs 2.366 Å). Although the distorting factor is unclear, we expect that it is due to the electrostatic repulsion between the positively charged hydrogen atoms of the indane C1 and the diaminoenol (magenta lines in Figure 3, H–H distance: 2.206 vs 2.210 Å for **3a** and **3b**).

In contrast, the increased enantioselectivity with **3d** is likely due to destabilization of the minor TS as the activation energy of the minor TS is higher for **3d** than that for **3b** (5.7 vs 4.3

TS$_{major}$ to give **2a**

TS$_{minor}$ to give *ent*-**2a**

Figure 3. Noncovalent Interaction Plot of the Transition States. The surfaces are colored on a blue–green–red scale according to strength of interaction. Blue indicates strong attractive interactions, green indicates weak attractive interactions, and red indicates strong repulsive interactions.

Table 5. Distortion/Interaction Analysis of the Transition State Geometries.[a]

TS	E_{act}	ΔE_{1a}	ΔE_{III}	E_{int}	O–H1	O–H7	H–H
3a TS$_{major}$	1.2 (16.4)	32.7 (32.7)	40.9 (41.8)	–72.4 (–58.1)	2.351	2.365	2.206
3a TS$_{minor}$	4.3 (16.3)	33.6 (33.6)	41.9 (43.3)	–71.2 (–60.6)	1.972	2.379	2.101
3b TS$_{major}$	0.9 (16.3)	32.5 (32.5)	40.7 (41.8)	–72.3 (–58.0)	2.360	2.366	2.210
3b TS$_{minor}$	4.3 (16.5)	33.6 (33.6)	42.2 (43.8)	–71.5 (–60.9)	1.967	2.390	2.101
3d TS$_{major}$	0.9 (16.2)	32.0 (32.0)	41.2 (42.2)	–72.3 (–58.0)	2.332	2.339	2.181
3d TS$_{minor}$	5.7 (17.8)	34.5 (34.5)	44.2 (45.7)	–73.0 (–62.4)	1.930	2.341	2.067

[a] Calculated at the B3LYP-D3/6-311+G**//B3LYP/6-31G* theoretical level. Energies in parentheses were without dispersion correction (B3LYP/6-311+G**//B3LYP/6-31G*). E_{act}, ΔE_{1a}, ΔE_{III}, and E_{int} stand for activation energy of step C (Figure 1), distortion energies of **1a** and the corresponding intermediate **III** (Figure 1), and interaction energy (in kcal/mol), respectively. O–H1, O–H7, and H–H stand for the distances (in Å) between the indane C1 H and the aldehyde O atoms, the indane C7 H and the diaminoenol O atoms, and the indane C1 H and the diaminoenol H atoms, respectively.

kcal/mol) while those of the major TS are the same (0.9 kcal/mol). That is, the enantioselectivity increased with **3d** because of slower production of *ent*-**2a** rather than faster production of **2a**. Interestingly, the interaction energy of the minor TS for **3d** is more stabilizing than that for **3b** (–73.0 vs –71.5 kcal/mol). Therefore, the main factor to destabilize the minor TS with **3d** is likely the distortion of intermediate **III** because the increase in distortion energy between **3b** and **3d** is larger for intermediate **III** than for the aldehyde (2.0 vs 0.9 kcal/mol). Again, the distorting factor of intermediate **III** is possibly the electrostatic repulsion between the indane C1 and the diaminoenol hydrogen atoms (H–H distance: 2.101 vs 2.067 Å for **3b** and **3d**). Actually, the distortion energies of intermediate **III** likely correlate with the H–H distances (40.7, 40.9, 41.2, 41.9, 42.2, and 44.2 kcal/mol with 2.210, 2.206, 2.181, 2.101, 2.101, and 2.067 Å, respectively).

To evaluate the significance of dispersion force, the energies were also calculated without dispersion corrections (B3LYP/6-311+G**//B3LYP/6-31G*) and presented in parentheses. It is noteworthy that the dispersion-correction decreased the interaction energies in the major TS more than those in the minor TS (14.3 vs 10.6 kcal/mol). This is in consistent with the result of NCI (Figure 3), where there are more green-colored surface, indicating existence of dispersion force, between the aldehyde and intermediate **III** in the major TS than in the minor TS. Obviously, dispersion force is more important in the major TS than in the minor TS.

To elucidate the reason for the lower enantioselectivities with the electron-poor benzaldehydes, TS calculations for the reaction of **1e** with **3b** were also performed. The free-energy difference between the TS to give **2e** and *ent*-**2e** was 1.09 kcal/mol, corresponding to 76% ee at 0 °C, at the B3LYP-D3/6-311+G**/PCM:dichloroethane//B3LYP/6-31G* theoretical level and thus in consistent with the observed decrease in enantioselectivity. The $\Delta G^{\ddagger}$ of the TS to give **2e** and *ent*-**2e** (7.5 and 8.6 kcal/mol) were lower by 0.44 and 0.51 kcal/mol than those to give **2a** and *ent*-**2a**, respectively, which indicate that the lower enantioselectivity is attributable to decreased destabilization in the minor TS. Although the TS geometries for **1e** are basically similar to those for **1a** (see SI for detail), the forming C–C bond length was found to be shorter in the TS to give *ent*-**2e** compared to that to give *ent*-**2a** (1.79 vs 1.82 Å). Probably, the destabilizing factor in the minor TS, *i.e.*, the electrostatic repulsion between the aryl groups, is reduced due to the lower electron density, which might be responsible for the observed lower enantioselectivities.

Conclusion

We demonstrated that the remote electronic tuning of NHC is effective for the catalytic asymmetric benzoin reaction. The NHC bearing remote electron-withdrawing substituents increased enantioselectivity of the reaction at the cost of the reaction rate. The remote electron-withdrawing substituents were also beneficial to prevent racemization of highly enolizable products. The results are consistent with the two conclusions that the rate-limiting step with triazolinylidene NHC is interchangeable as in the reaction with thiazolinylidene,[5] and that the remote electronic effect is operative as we previously proposed.[43–45,49] DFT calculations and NCI analysis confirmed that the origin of the enantioselectivity is the orientation of the aldehyde aryl group with respect to the diaminoenol aryl group in the C–C bond forming TS as proposed in the literature. Moreover, the distortion/interaction analysis suggested that the distortion of the diaminoenol intermediate moieties of the TS caused by the remote electron-withdrawing substituents could be responsible for the increased enantioselectivity.

Experimental Section

Typical procedure for Tables 1–3 (Table 1, entry 5). Benzoin (2a): NHC precatalyst **3e** (5.91 mg, 10 µmol) was placed in a flask and the flask was evacuated and filled with argon ten times. Then a solution of proton sponge (2.3 mg, 10 µmol) in distilled ClCH$_2$CH$_2$Cl (1.0 mL) was added, and the resulting solution was stirred at 30 °C. After 1 h, the solution was cooled at 0 °C, and aldehyde **1a** (0.10 mL, 1.0 mmol) was added via syringe. The solution was then stirred at the same temperature for 1 h, and the whole solution was directly purified by silica gel column chromatography (hexane/EtOAc = 8:1 to 3:1) to give **2a** (30.7 mg, 0.29 mmol, 29% yield) as a white solid of mp 132–133 °C with $[\alpha]_D^{17}$ +163 (*c* 1.00, CH$_3$OH). The ee was determined to be 95% ee by HPLC analysis (COSMOSIL CHiRAL 3A; hexane/*i*-PrOH 9:1; 0.5 mL/min; 254 nm; 24.4 min (*R*) and 28.1 min (*S*)). The absolute configuration was assigned to be (*S*) by comparing the sign of the specific rotation with that reported in literature (mp 131–132 °C;[16] $[\alpha]_D^{rt}$ −108.4 (*c* 1, CH$_3$OH) for (*R*)-**2a** with 75% ee[8]). ^{1}H NMR (400 MHz, CDCl$_3$): δ 4.55 (d, *J* = 6.0 Hz, 1H), 5.95 (d, *J* = 6.0 Hz, 1H), 7.27–7.33 (m, 5H), 7.40 (t, *J* = 7.5 Hz, 2H), 7.52 (t, *J* = 7.5 Hz, 1H), 7.92 (d, *J* = 7.0 Hz, 2H). The ^{1}H NMR was identical to that reported.[54]

Supporting Information

Additional references cited within the Supporting Information.[55–63]

Acknowledgements

[1]   Originally reported as a cyanide-catalyzed reaction: A. J. Lapworth, *J. Chem. Soc.* **1903**, *20*, 995–1005.
[2]   T. Ukai, R. Tanaka, S. Dokawa, *J. Pharm. Soc. Jpn.* **1943**, *63*, 296–300.
[3]   Breslow, R. *J. Am. Chem. Soc.* **1958**, *80*, 3719–3726.
[4]   Y.-T. Chen, G. L. Barletta, K. Haghjoo, J. T. Cheng, F. Jordan, *J. Org. Chem.* **1994**, *59*, 7714–7722.
[5]   M. J. White, F. J. Leeper, *J. Org. Chem.* **2001**, *66*, 5124–5131.
[6]   A. Berkessel, S. Elfert, V. R. Yatham, J-M. Neudörfl, N. E. Schlörer, J. H. Teles, *Angew. Chem. Int. Ed.* **2012**, *51*, 12370–12374.
[7]   J. C. Sheehan, D. H. Hunneman. *J. Am. Chem. Soc.* **1966**, *88*, 3666–3667.
[8]   D. Enders, K. Breuer, *Helv. Chim. Acta.* **1996**, *79*, 1217–1221.

[9]   C. A. Dvorak, V. H. Rawal, *Tetrahedron Lett.* **1988,** *39*, 2925–2928.

[10]   R. L. Knight, F. J. Leeper, *J. Chem. Soc., Perkin Trans. 1*, **1998**, 1891–1893.

[11]   D. Enders, U. Kallfass, *Angew. Chem. Int. Ed.* **2002**, *41*, 1743–1745.

[12]   J. Pesch, K. Harms, T. Bach, *Eur. J. Org. Chem.* **2004**, 2025–2035.

[13]   Y. Tachibana, N. Kihara, T. Takata, *J. Am. Chem. Soc.* **2004**, *126*, 3438–3439.

[14]   Y. Ma, S. Wei, J. Wu, F, Yang, B. Liu, J. Lan, S. Yang, J. You, *Adv. Synth. Catal.*, **2008**, *350*, 2645–2651.

[15]   S. E. O'Toole, S. J. Connon, *Org. Biomol. Chem.*, **2009**, 7, 3584–3593.

[16]   L. Baragwanath, C. A. Rose, K. Zeitler, S. J. Connon, *J. Org. Chem.* **2009**, *74*, 9214–9217.

[17]   J. P. Brand, J. Ignacio, O. Siles, J. Waser, *Synlett,* **2010**, 881–884.

[18]   T. Soeta, Y. Tabatake, K. Inomata, Y. Ukaji, *Tetrahedron* **2012**, *68*, 894–899.

[19]   Z. Rafiński, *Tetrahedron* **2016**, *72*, 1860–1867.

[20]   G. Delany, S. J. Connon, *Org. Biomol. Chem.* **2021**, *19*, 248–258.

[21]   H. Takikawa, H. Hachisu, J. W. Bode, K. Suzuki, *Angew. Chem. Int. Ed.* **2006**, *45*, 3492–3494.

[22]   H. Takikawa, S. Suzuki, K. *Org. Lett.* **2007**, *9*, 2713–2716.

[23]   K. P. Stockton, B. W. Greatrex, D. K. Taylor, *J. Org. Chem.* **2014**, *79*, 5088–5096.

[24]   B. Kang, T. Sutou, Y. Wang, S. Kuwano, Y. Yamaoka, K. Takasu, K. Yamada, *Adv. Synth. Catal.* **2015**, *357*, 131–147.

[25]   K. Hermández, T. Parella, J. Joglar, J. Bujons, M. Pohl, and P. Clapés, *Chem. Eur. J.* **2015**, *21*, 3335–3346.

[26]   B. Kang, Y. Wang, S. Kuwano, Y. Yamaoka, K. Takasu, K. Yamada, *Chem Commun.* **2017**, *53*, 4469–4472.

[27]   S. Sato, K. Sakata, Y. Hashimoto, H. Takikawa, K. Suzuki, *Angew. Chem. Int. Ed.* **2017**, *56*, 12608–12613.

[28]   Parmar, P. Haghshenas, M. Gravel, *Org. Lett.* **2021**, *23*, 1416–1421.

[29]   T. Inokuma, K. Masui, K. Fukuhara, K. Yamada, *Chem. Eur. J.* **2023**, *29*, e202203120.

[30]   K. Yamasaki, A. Yamauchi, T. Inokuma, Y. Miyakawa, Y. Wang, R. Oriez, Y. Yamaoka, K. Takasu, N. Tanaka, Y. Kashiwada, K. Yamada, *Asian J. Org. Chem.* **2021**, *10*, 1828–1834

[31]   T. Inokuma, T. Sakakibara, T. Someno, K. Masui, A. Shigenaga, A. Otaka, K. Yamada, *Chem. Eur. J.* **2019**, *25*, 13829–13832.

[32]   H. Kiyama, T. Inokuma, Y. Kuroda, Y. Yamaoka, K. Takasu, K. Yamada, K. *Tetrahedron Lett.* **2019**, *60*, 175–177.

[33]   T. Jichu, T. Inokuma, K. Aihara, T. Kohiki, K. Nishida, A. Shigenaga, K. Yamada, A. Otaka, *ChemCatChem* **2018**, *10*, 3402–3405.

[34]   T. Inokuma, K. Nishida, A. Shigenaga, K. Yamada, A. Otaka, *Heterocycles* **2018**, *97*, 1269–1287.

[35]   Y. Wang, R. Oriez, S. Oh, Y. Miyakawa, Y. Yamaoka, K. Takasu, K. Yamada, *Heterocycles* **2017**, *95*, 314–321.

[36]   Y. Kuroda, S. Harada, A. Oonishi, H. Kiyama, Y. Yamaoka, K. Yamada, K. Takasu, *Angew. Chem. Int. Ed.* **2016**, *55*, 13137–13141.

[37]   K. Yamada, A. Oonishi, Y. Kuroda, S. Harada, H. Kiyama, Y. Yamaoka, K. Takasu, *Tetrahedron Lett.* **2016**, *57*, 4098–4100.

[38]   Y, Wang, R. Oriez, S. Kuwano, Y. Yamaoka, K. Takasu, K. Yamada, *J. Org. Chem.* **2016**, *81*, 2652–2664

[39]   Y. Kuroda, S. Harada, A. Oonishi, Y. Yamaoka, K. Yamada, K. Takasu, K. *Angew. Chem. Int. Ed.* **2015**, *54*, 8263–8266.

[40]   S. Harada, S. Kuwano, Y. Yamaoka, K. Yamada, K. Takasu, *Angew. Chem. Int. Ed.* **2013**, *52*, 10227–10230.

[41]   S. Kuwano, S. Harada, R. Oriez, K. Yamada, *Chem. Commun.* **2012**, *48*, 145–147

[42]   M. S. Kerr, J. Read de Alaniz, T. Rovis, *J. Am. Chem. Soc.* **2002**, *124*, 10298–10299.

[43]   S. Kuwano, S. Harada, B. Kang, R. Oriez, Y. Yamaoka, K. Takasu, K. Yamada, *J. Am. Chem. Soc.* **2013**, *135*, 11485–11488.

[44]   Y. Wang, A. Yamauchi, K. Hashimoto, T. Fujiwara, T. Inokuma, Y. Mitani, K. Ute, S. Kuwano, Y. Yamaoka, K. Takasu, K. Yamada, *ACS Catal.* **2022**, *12*, 6100–6107.

[45]   K. Yamada, A. Yamauchi, T. Fujiwara, K. Hashimoto, Y. Wang, S. Kuwano, T. Inokuma, *Asian J. Org. Chem.* **2022**, *11*, e202200452.

[46]   J. Read de Alaniz, T. Rovis, T. *J. Am. Chem. Soc.* 2005, *127*, 6284–6289.

[47]   J. Mahatthananchai, J. W. Bode, *Chem. Sci.* **2012**, *3*, 192–197.

[48]   C. J. Collett, R. S. Massey, O. R. Maguire, A. S. Batsanov, A.M. C. O'Donoghue, A. D. Smith, *Chem. Sci.* **2013**, *4*, 1514–1522.

[50]   T. Ema, Y. Nanjo, S. Shiratori, Y. Terao, R. Kimura, *Org. Lett.* **2016**, *18*, 5764–5767.

[51]   T. Dudding, K. N. Houk, *Proc. Natl. Acad. Sci. USA* **2004**, *101*, 5770–5775.

[52]   E. R. Johnson, S. Keinan, P. Mori-Sánchez, J. Contreras-García, A. J. Cohen, W. Yang, *J. Am. Chem. Soc.* **2010**, *132*, 6498–6506.

[53]   F. M. Bickelhaupt, K. N.; Houk, *Angew. Chem. Int. Ed.* **2017**, *56*, 10070–10086.

[54]   M. Baranac-Stojanović, R. Marković, M. Stojanović, *Tetrahedron* **2011**, *67*, 8000–8008.

[55]   M. S. Kerr, J. Read de Alaniz, T. Rovis, *J. Org. Chem.* **2005**, *70*, 5725–5728.

[56]   G. D. Carmine, D. Ragno, O. Bortolini, P. P. Giovannini, A. Mazzanti, A. Massi, M. Fogagnolo, *J. Org. Chem.* **2018**, *83*, 2050–2057.

[57]   P. Singh, A. Mittal, S. Kumar, *Bioorg. Med. Chem.* **2007**, *15*, 3990–3996.

[58]   Y. Liu, X. Xu, Y. Zhang, *Tetrahedron* **2004**, *22*, 4867–4873.

[59]   V. Dhayalan, S. C. Gadekar, Z. Alassad, A. Milo, *Nat. Chem.* **2019**, *11*, 543–551.

[60]   U. R. Seo, Y. K. Chung, *RSC Adv.* **2014**, *4*, 32371–32374.

[61]   L. Lin, X. Bai, X. Ye, X. Zhao, C.-H. Tan, Z. Jiang, *Angew. Chem. Int. Ed.* **2017**, *56*, 13842–13846.

[62]   B. Deppmeier, A. Driessen, T. Hehre, W. Hehre, P. Klunzinger, S. Ohlinger, J. Schnitker, Spartan'18 Wavefunction, Inc. Irvine, CA.

[63]   M. J. Frisch, G. W. Trucks, H. B. Schlegel, G. E. Scuseria, M. A. Robb, J. R. Cheeseman, G. Scalmani, V. Barone, G. A. Petersson, H. Nakatsuji, X. Li, M. Caricato, A. Marenich, J. Bloino, B. G. Janesko, R. Gomperts, B. Mennucci, H. P. Hratchian, J. V. Ortiz, A. F. Izmaylov, J. L. Sonnenberg, D. Williams-Young, F. Ding, F. Lipparini, F. Egidi, J. Goings, B. Peng, A. Petrone, T. Henderson, D. Ranasinghe, V. G. Zakrzewski, J. Gao, N. Rega, G. Zheng, W. Liang, M. Hada, M. Ehara, K. Toyota, R. Fukuda, J. Hasegawa, M. Ishida, T. Nakajima, Y. Honda, O. Kitao, H. Nakai, T. Vreven, K. Throssell, J. A. Montgomery, Jr., J. E. Peralta, F. Ogliaro, M. Bearpark, J. J. Heyd, E. Brothers, K. N. Kudin, V. N. Staroverov, T. Keith, R. Kobayashi, J. Normand, K. Raghavachari, A. Rendell, J. C. Burant, S. S. Iyengar, J. Tomasi, M. Cossi, J. M. Millam, M. Klene, C. Adamo, R. Cammi, J. W. Ochterski, R. L. Martin, K. Morokuma, O. Farkas, J. B. Foresman, D. J. Fox, Gaussian, Inc., Wallingford CT, **2016**.

Entry for the Table of Contents
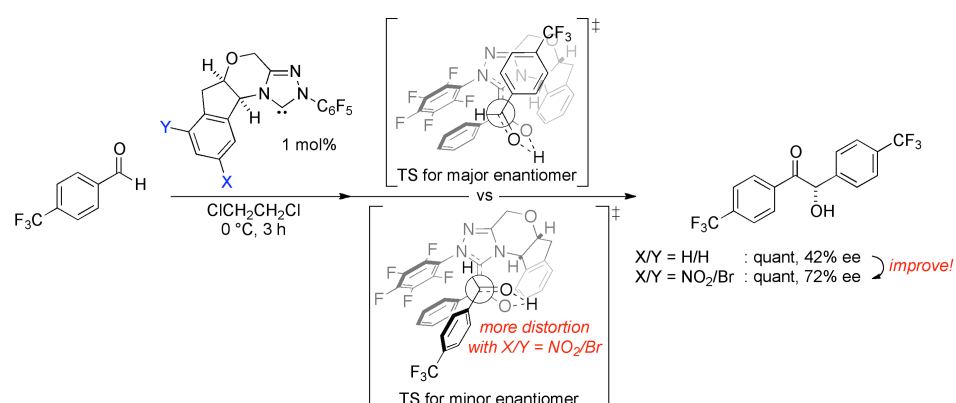
The introduction of remote electron-withdrawing groups in N-heterocyclic carbene catalyst increased enantioselectivity of the benzoin reaction at the cost of the reaction rate. The increased enantioselectivity was rationalized by DFT calculations with noncovalent-interaction and distortion/interaction-energy analyses.